

Photoionization of optically trapped ultracold atoms with a high-power light-emitting diode

Simone Götz, Bastian Höltkemeier, Thomas Amthor, and Matthias Weidemüller

Citation: *Rev. Sci. Instrum.* **84**, 043107 (2013); doi: 10.1063/1.4795475

View online: <http://dx.doi.org/10.1063/1.4795475>

View Table of Contents: <http://rsi.aip.org/resource/1/RSINAK/v84/i4>

Published by the [American Institute of Physics](http://www.aip.org).

Additional information on *Rev. Sci. Instrum.*

Journal Homepage: <http://rsi.aip.org>

Journal Information: http://rsi.aip.org/about/about_the_journal

Top downloads: http://rsi.aip.org/features/most_downloaded

Information for Authors: <http://rsi.aip.org/authors>

ADVERTISEMENT

physicstoday

Comment on any
Physics Today article.

Measured energy in Japan
David von Seggern
(rvseg@seismo.unr.edu) University of Nevada
July 2012, page 10
DIGITAL OBJECT IDENTIFIER
<http://dx.doi.org/10.1063/PT.3.1619>

Comment on this article
By the act of hitting a ball with a bat, one calculates the force energy to deliver the ball to its new location, but one must also take into account that the ball extended its energy release to that which became struck by the ball as its momentum ceased and passed energy to the struck team. Therefore the parameters of the damage extend into the future when the received energy to that pushed upon, later becomes released in a new event. Perhaps calculations of one added that in while another's calculations did not. E.M.C.
Written by Edgar Mocarvill, 14 July 2012 19:59

Photoionization of optically trapped ultracold atoms with a high-power light-emitting diode

Simone Götz, Bastian Höltkemeier, Thomas Amthor,^{a)} and Matthias Weidemüller^{b)}

Physikalisches Institut, Universität Heidelberg, Im Neuenheimer Feld 226, 69120 Heidelberg, Germany

(Received 12 October 2012; accepted 3 March 2013; published online 17 April 2013)

Photoionization of laser-cooled atoms using short pulses of a high-power light-emitting diode (LED) is demonstrated. Light pulses as short as 30 ns have been realized with the simple LED driver circuit. We measure the ionization cross section of ^{85}Rb atoms in the first excited state, and show how this technique can be used for calibrating efficiencies of ion detector assemblies. © 2013 American Institute of Physics. [<http://dx.doi.org/10.1063/1.4795475>]

I. INTRODUCTION

The availability of high-power light-emitting diodes (LEDs) covering a vast range of wavelengths allows one to replace sophisticated laser sources in a large number of applications, whenever the coherence properties of the light source are not needed. In pulsed mode, LEDs can be operated with currents exceeding their continuous mode damage threshold. Thus, short duration pulses with very high intensities can be created. This allows their use in different kinds of imaging techniques, such as flow velocimetry,¹ where the light intensities in continuous mode operation are insufficient. LEDs are also increasingly used in atomic and molecular physics where they replace the so-far indispensable lasers in a growing number of fields. One example is light-induced atom desorption (LIAD) of atoms from surfaces, which can be applied for fast and efficient loading of magneto-optical traps (MOT).^{2–6} Another example is the photoionization of atoms in a laser-cooled gas for the creation of ultracold ions. Cetina *et al.* have used an LED at 370 nm to photoionize a large number of Yb atoms from a MOT in order to transfer the cold ions efficiently into a surface-electrode ion trap.⁷

Pulsed photoionization of atoms trapped in a MOT with ultrashort laser pulses has been employed to create short ion pulses with a well-defined momentum⁸ and arbitrarily shaped high-coherence electron bunches.⁹ In this article, we report on substituting pulsed laser sources by a high-power LED in pulsed mode of operation. The short ion pulses generated by this technique can be used to calibrate time-of-flight assemblies with high accuracy. Furthermore, the photoionization with LEDs can be applied for measurements of atomic and molecular ionization cross sections.

II. SETUP

The ionization light pulses are produced by a blue high-power LED from CREE (model XLamp XR-E LED XREBLU-B5¹⁰). The spectrum of the emitted light, measured with a fiber-optic spectrometer (Ocean Optics, model USB2000), is shown in Fig. 1. The central wavelength is at

480 nm and the spectral width is 28 nm (FWHM). As can be seen from the level scheme in the inset in Fig. 1, Rb atoms which are excited into the $5P_{3/2}$ state can either reach ionization continuum or be excited to Rydberg states by the LED. In our case, 50% of the spectral light distribution has a photon energy above the ionization threshold.

The LED is mounted on a heat sink, which is attached to a mirror mount for fine adjustment. It can be operated either in continuous mode using a conventional regulated DC current source, or in pulsed mode with short current pulses produced by the driver circuit depicted in Fig. 2. At the input of the pulse driver, a low transistor-transistor logic (TTL) pulse is applied. The inverting MOSFET driver SN75372 provides the gate voltage for the switching power MOSFET IRFU3910. The additional Schottky diode D1 is needed for damping voltage overshoots and ringing. Capacitor C1 provides the energy for the light pulse. Resistor R1 = 0.1 Ω is used to limit the current and to allow for a measurement of the current with a differential probe. In this configuration, a maximum current of 2 A flows through the LED during the pulse. As the specified maximum current for continuous operation of the LED is 1000 mA, the pulse width and duty cycle must be chosen carefully in order not to destroy the LED.

The light emitted by the diode is divergent with an opening angle of the light cone of $\theta = 100^\circ$ (FWHM of luminous intensity). The emitted light is imaged onto the atom cloud at a distance of 41 cm using an aspheric lens with a diameter of 60 mm and a focal length of 40 mm, which is placed 12 cm from the LED. The intensity distribution at the image plane has been measured using a power meter behind a movable iris with an aperture of 1.5 mm. The intensity distribution I_{LED} is constant within 10% over an area of about $20 \times 20 \text{ mm}^2$, which typically covers the area of a trapped atom cloud.

The setup used to demonstrate the pulsed LED ion source is designed to detect recoil ions from collisions in a MOT on a micro-channel plate (MCP) followed by a position sensitive detector. The MOT is therefore placed inside a recoil-ion momentum spectrometer^{11,12} (Fig. 3). The atoms are loaded from an additional two-dimensional MOT¹³ (not shown in the picture). Typically 8×10^7 atoms are trapped in the main retro-reflected MOT at a density of 10^{10} cm^{-3} . A detailed description of the apparatus can be found in Ref. 14. When shining the light from the LED onto the MOT, the ions produced by

^{a)}Present address: Philips Technologie GmbH, Research Laboratories, Röntgenstr. 24-26, 22335 Hamburg, Germany.

^{b)}weidemueller@uni-heidelberg.de.

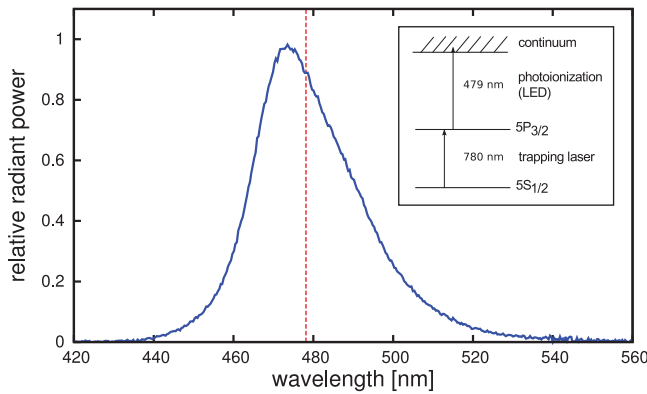


FIG. 1. Spectrum of the LED. The red dotted line indicates the ionization threshold of Rb atoms in the first excited $5P_{3/2}$ state. Inset: Level scheme of ^{85}Rb .

photoionization are accelerated towards and focused onto the ion detector by an electric field of 0.3 V/cm, followed by a field-free drift region. After a time of flight of 315 μs , they are detected by a micro-channel plate. In order to avoid background ions, the ion detector is gated for 4.5 μs with a delay of 314.5 μs after the LED pulse.

III. RESULTS

A. Continuous mode

While running the LED in continuous mode, the fluorescence signal of the MOT is monitored with and without the LED light present ($\Gamma_{\text{PI}} = 0$). In order to convert the fluorescence signal into the number of trapped atoms, the fluorescence is calibrated using standard absorption imaging of the atomic cloud.¹⁵ As clearly seen in Fig. 4, the loss of atoms from the trap induced by photoionization results in a decrease in the total atom number in the trap. We verified that only the excited atoms are ionized by measuring the ion rate on the MCP with and without the trapping lasers, finding no signal in the latter case.

Following Townsend *et al.*,¹⁶ we estimate the fraction of the trapped atoms in the excited state to be $f_{\text{exc}} = 0.4$ for our MOT laser settings (20 mm $1/e^2$ beam diameter, 73 mW total laser power on the cooling transition). Under these condi-

tions, the photoionization rate (per atom) can be expressed as $\Gamma_{\text{PI}} = f_{\text{exc}} \mathcal{N} \sigma$ where \mathcal{N} denotes the photon flux of the light source at energies larger than the ionization threshold, given by the spectral intensity distribution in Fig. 1. σ is the effective ionization cross section for the part of the spectrum of the LED being above the ionization threshold. For the following analysis, we assume σ to be constant over the LED spectrum. Previous measurements^{17–19} and calculations²⁰ only show a small variation below 10% of the cross section over this spectral range justifying this assumption. The effective cross section can be determined from the total number of trapped atoms $N(t)$ using a simple rate equation model:²¹

$$N(t) = \frac{L}{\Gamma'} (1 - e^{-\Gamma' t}) \quad (1)$$

with L being the atom loading rate into the trap and $\Gamma' = \Gamma_{\text{PI}} + \Gamma_{\text{at}}$ the total loss rate (per atom). The rate Γ_{at} accounts for intrinsic atom loss from the trap, e.g., due to collisions with hot background atoms. From a fit of Eq. (1) to the loading curve without the LED light present, L and Γ_{at} can be determined (see Fig. 4). Using these values and measuring the loading curve with the LED light on, σ can be determined from Γ_{PI} .

During the experiment, we vary the intensity of the LED from $I_{\text{LED}} = 190 \text{ W/m}^2$ to $I_{\text{LED}} = 370 \text{ W/m}^2$, corresponding to a photon flux of $\mathcal{N} = 4.6 \times 10^{20} \text{ s}^{-1} \text{ m}^{-2}$ and $\mathcal{N} = 8.9 \times 10^{20} \text{ s}^{-1} \text{ m}^{-2}$, respectively. Only photons with an energy above the ionization energy have been included in the photon flux. We deduce an averaged photoionization cross section of $\sigma = (6.8 \pm 1.2) \times 10^{-18} \text{ cm}^2$, where the given error is statistical. A systematic error of roughly 50% adds to the statistical error, arising from the uncertainty in the determination of the total atom number and the excited state fraction. To reduce this error, a better calibration of the absorption imaging system, e.g., using saturated absorption imaging,^{22,23} would be required, but is beyond the scope of this paper.

B. Pulsed mode

Operating the LED in pulsed mode, the rate of measured ions can be expressed as

$$R_{\text{ion}} = N \Gamma_{\text{PI}} \eta. \quad (2)$$

N is the total atom number in the cloud and the factor η denotes the detector efficiency ($\eta \approx 30\%$). The ion rate is measured by counting the number of ions detected by the MCP. After the time of flight of 314 μs , which the recoil ions need to travel from the interaction region to the MCP, a gate is applied to the MCP signal. Since the overall background ion rate is as low as 20 Hz, setting the gate to 7 μs results in a complete suppression of background signal.

With a repetition rate of 100 Hz and a pulse length of 100 ns, leading to $\mathcal{N} = 5.9 \times 10^{11} \text{ s}^{-1} \text{ m}^{-2}$, we observe a rate of 88 Hz. Reducing the pulse length to 30 ns while keeping the repetition rate constant, corresponding to $\mathcal{N} = 9.6 \times 10^{10} \text{ s}^{-1} \text{ m}^{-2}$, the ion rate decreases to 9 Hz. The non-linearity between the ion count rate and the intensity is due to atom number fluctuations in the trap. From these

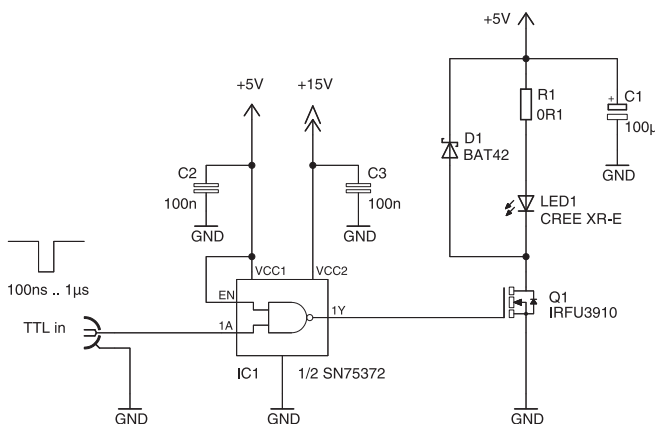


FIG. 2. Circuit diagram of the pulsed LED. For explanation see text.

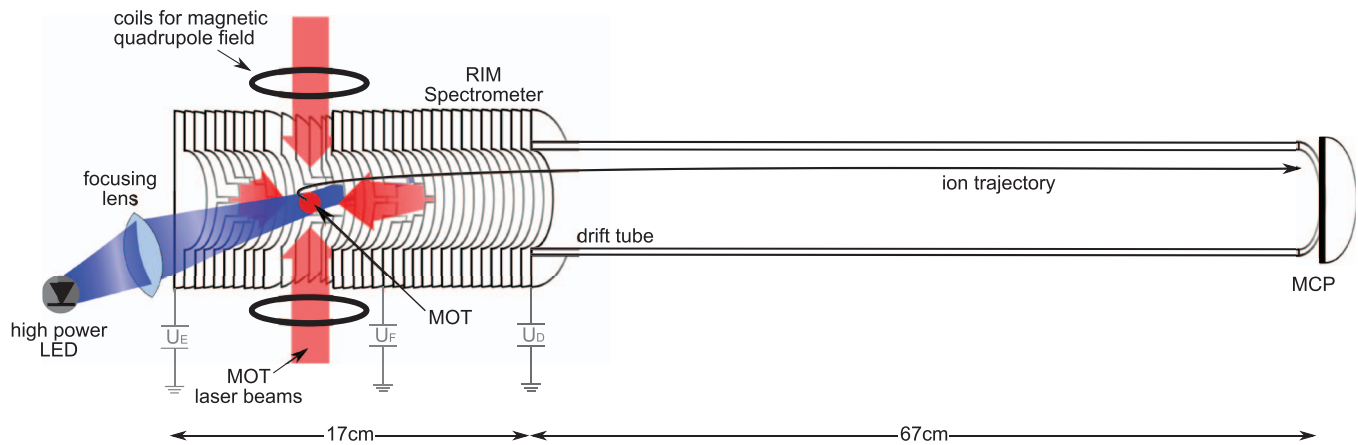


FIG. 3. Schematics of the experimental setup. Rb atoms are trapped in a magneto-optical trap in the center of a recoil-ion momentum spectrometer and ionized by the light emitted from the LED, which is imaged onto the atom cloud. The aspherical imaging lens has a focal length $f = 40$ mm. The ions are accelerated towards the MCP detector by the voltage U_E and focused in time by the voltage U_F before entering the field free drift region with the voltage $U_D = 0$.

measurements, we deduce an averaged cross section of $\sigma = (8.8 \pm 2.2) \times 10^{-18} \text{ cm}^2$.

C. Discussion

The effective cross sections measured in continuous and pulsed mode both match well within the statistical error bars. Previously published results are all based on photoionization using narrow-bandwidth lasers. The measured cross sections covered a spectral range from 406.1 nm to 476.5 nm.^{17–19,21} Our measured cross section compares favourably to the values measured in Refs. 17–19 and the calculations in Ref. 20, but deviates by a factor of two from the value measured by Gabbanini *et al.*²¹

We further explore the possibility of using the described setup as a source of short ion pulses. For this purpose, the LED is operated in pulsed mode. The resulting time of flight distribution of the produced ion pulses, detected by the MCP after a time of flight of 315 μs , is depicted in Fig. 5. Due to

the maximum recoil momentum of $0.7 \mu\text{eV}$ which the ions acquire during the ionization process and the imperfect time focusing of the recoil ion momentum spectrometer the ions' time of flight distribution is broadened to 190 ns and 300 ns (FWHM) after ionization with 30 ns and 100 ns pulses, respectively. A Wiley McLaren type of spectrometer²⁴ could be used to reduce the temporal broadening of the ion pulses. In this type of spectrometer, the geometry as well as the focusing voltage are optimized for time of flight focusing only, whereas the geometry and focusing voltages of a recoil ion spectrometer as used in this paper are a compromise between time of flight resolution and spatial resolution. The length of the ion pulses is limited by the finite rise time of the LED, which means that at even shorter pulse lengths the total ion flux will decrease significantly. Whenever shorter ion pulses are needed, the use of pulsed laser sources will be necessary. However, as we have demonstrated LEDs offer a cost effective alternative for pulse lengths of a few nanoseconds and beyond.

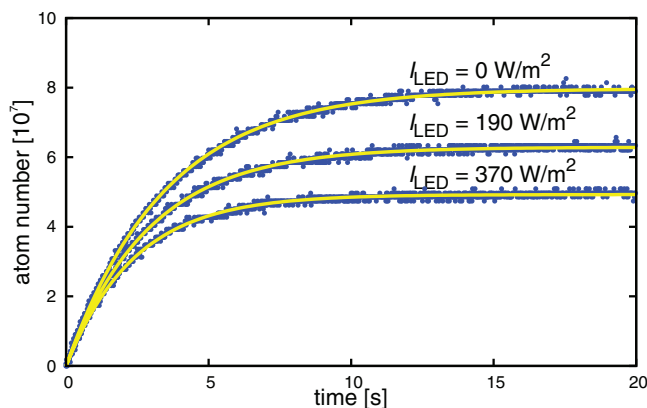


FIG. 4. Loading curve of MOT with and without the LED. The data points correspond to the fluorescence signal converted into a total number of trapped atoms. The yellow solid lines are a fit of Eq. (1). The intensity of the LED are $I_{\text{LED}} = 190 \text{ W/m}^2$ and $I_{\text{LED}} = 370 \text{ W/m}^2$, measured at the position of the atom cloud.

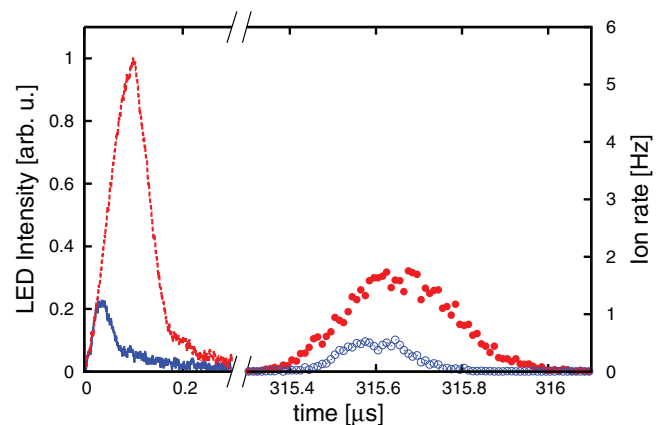


FIG. 5. Measurement of temporal intensity distributions of the LED in pulsed mode. The LED is pulsed for 30 ns (blue solid curve) or 100 ns (red dashed curve). After a time of flight of 315 μs the ions are detected and have a time spread of 190 ns (blue open circles) and 300 ns (red solid circles) (FWHM), respectively.

IV. CONCLUSION

We have demonstrated a simple and low-cost ionizing light source based on a high-power LED, which can be used to replace sophisticated laser sources whenever the coherence properties of the light source are not an issue. High-power LEDs are nowadays available for a vast range of different wavelengths. The length of the light pulses is mainly limited by the parasitic capacitance of the LED. We have realized LED pulses as short as 30 ns. The effective photoionization cross section σ is determined from two independent measurements ionizing magneto-optically trapped atoms from the excited state, using the LED in cw mode and in pulsed mode, to be $\sigma = (6.8 \pm 1.2) \times 10^{-18} \text{ cm}^2$ and $\sigma = (8.8 \pm 2.2) \times 10^{-18} \text{ cm}^2$, respectively. Using additional spectral filters, the exact dependence of the ionization cross-section on the wavelength could be measured. Conversely, for a well-known photoionization cross section, an LED operated in pulsed mode can be employed to precisely determine the detector efficiency or excited state fraction. This always implies that either one of these two values is well known, otherwise only their product can be determined. In our experiment, we apply photoionization with pulsed LEDs for routinely calibrating the time-of-flight spectrometer, replacing a pulsed lasers, which has been employed so far. With our setup, we have detected ion pulses as short as 190 ns, with the measured pulse length being limited by the instrument's resolution. Polarizing the light from the LED to induce a characteristic angular distribution of the recoil ions, one could also use the setup for calibration of position resolving detectors as used, e.g., in recoil-ion momentum spectrometers.^{25,26}

ACKNOWLEDGMENTS

We acknowledge financial support by the BMBF within the framework of "FAIR-SPARC" (Contract No. 06HD9131I) and the Heidelberg Center for Quantum Dynamics. B.H. acknowledges support by the GSI Helmholtzzentrum für Schwerionenforschung and HGS-Hire.

¹C. Willert, B. Stasicki, J. Klinner, and S. Moessner, *Meas. Sci. Technol.* **21**, 075402 (2010).

- ²B. P. Anderson and M. A. Kasevich, *Phys. Rev. A* **63**, 023404 (2001).
- ³S. N. Atutov, R. Calabrese, V. Guidi, B. Mai, A. G. Rudavets, E. Scansani, L. Tomassetti, V. Biancalana, A. Burchianti, C. Marinelli, E. Mariotti, L. Moi, and S. Veronesi, *Phys. Rev. A* **67**, 053401 (2003).
- ⁴C. Klempt, T. van Zoest, T. Henninger, O. Topic, E. Rasel, W. Ertmer, and J. Arlt, *Phys. Rev. A* **73**, 013410 (2006).
- ⁵G. Telles, T. Ishikawa, M. Gibbs, and C. Raman, *Phys. Rev. A* **81**, 032710 (2010).
- ⁶E. Mimoun, L. D. Sarlo, D. Jacob, J. Dalibard, and F. Gerbier, *Phys. Rev. A* **81**, 023631 (2010).
- ⁷M. Cetina, A. Grier, J. Campbell, I. Chuang, and V. Vuletić, *Phys. Rev. A* **76**, 041401 (2007).
- ⁸M. P. Reijnders, P. A. van Kruisbergen, G. Taban, S. B. van der Geer, P. H. A. Mutsaers, E. J. D. Vredenburg, and O. J. Luiten, *Phys. Rev. Lett.* **102**, 034802 (2009).
- ⁹A. J. McCulloch, D. V. Sheludko, S. D. Saliba, S. C. Bell, M. Junker, K. A. Nugent, and R. E. Scholten, *Nat. Phys.* **7**, 785 (2011).
- ¹⁰See <http://www.cree.com> for the datasheet of the used LED.
- ¹¹J. Ullrich, R. Moshhammer, R. Dörner, O. Jagutzki, V. Mergel, H. Schmidt-Böcking, and L. Spielberger, *J. Phys. B* **30**, 2917 (1997).
- ¹²R. Dörner, V. Mergel, O. Jagutzki, L. Spielberger, J. Ullrich, R. Moshhammer, and H. Schmidt-Böcking, *Phys. Rep.* **330**, 95 (2000).
- ¹³K. Dieckmann, R. J. C. Spreeuw, M. Weidemüller, and J. T. M. Walraven, *Phys. Rev. A* **58**, 3891 (1998).
- ¹⁴S. Götz, B. Höltekemeier, C. Hofmann, D. Litsch, B. DePaola, and M. Weidemüller, *Rev. Sci. Instrum.* **83**, 073112 (2012).
- ¹⁵W. Ketterle, D. S. Durfee, and D. M. Stamper-Kurn, "Making, probing and understanding Bose-Einstein condensates," in *Proceedings of the international school of Physics "Enrico Fermi" course CXL Bose-Einstein condensation in atomic gases* (IOS, Amsterdam, Netherlands, 1999), pp. 95–113.
- ¹⁶C. G. Townsend, N. H. Edwards, C. J. Cooper, K. P. Zetie, C. J. Foot, A. M. Steane, P. Szriftgiser, H. Perrin, and J. Dalibard, *Phys. Rev. A* **52**, 1423 (1995).
- ¹⁷A. I. Klyucharev and V. Y. Sepman, *Opt. Spectrosc.* **712**, 38 (1975).
- ¹⁸T. Dinneen, C. Wallace, K. Tan, and P. Gould, *Opt. Lett.* **17**, 1706 (1992).
- ¹⁹H. Wei, R. Ya-Ping, J. Feng-Dong, Z. Yin-Peng, L. Long-Wei, D. Xing-Can, X. Ping, X. Xiang-Yuan, and Z. Zhi-Ping, *Chin. Phys. Lett.* **29**, 013201 (2012).
- ²⁰I. Petrov, V. Sukhorukov, E. Leber, and H. Hotop, *Eur. Phys. J. D* **10**, 53 (2000).
- ²¹C. Gabbanini, S. Gozzini, and A. Lucchesini, *Opt. Commun.* **141**, 25 (1997).
- ²²S. L. Winoto, M. T. DePue, N. E. Bramall, and D. S. Weiss, *Phys. Rev. A* **59**, 19 (1999).
- ²³M. T. DePue, S. L. Winoto, D. J. Han, and D. S. Weiss, *Opt. Commun.* **180**, 73 (2000).
- ²⁴W. C. Wiley and I. H. McLaren, *Rev. Sci. Instrum.* **26**, 1150 (1955).
- ²⁵S. Wolf and H. Helm, *Phys. Rev. A* **56**, R4385 (1997).
- ²⁶S. Wolf and H. Helm, *Phys. Rev. A* **62**, 043408 (2000).